



Journal of Applicable Chemistry

2018, 7 (5): 1231-1237

(International Peer Reviewed Journal)



Synthesis of Flower like Monoclinic Zirconia: Its Structural, Photoluminescence and Latent Finger Print Studies

L. Parashuram^{1,2}, S. Sreenivasa^{1*} and S. Akshatha¹

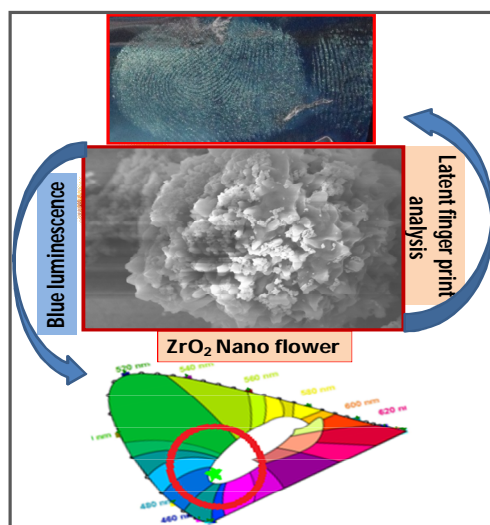
1. Department of Studies and Research in Organic Chemistry, Tumkur University, Tumkur-572101, **INDIA**
2. Department of Chemistry, New Horizon College of Engineering, Affiliated to VTU, Bangalore-560087, **INDIA**
Email: drsreenivasa@yahoo.co.in

Accepted on 16th September, 2018

ABSTRACT

Flower like zirconia nanomaterial was prepared by simple precipitation technique under high dilution conditions. The material prepared and calcinated at 400°C exhibited monoclinic phase. The FTIR spectra showed an intense peak at 749 cm^{-1} , which is the characteristic peak of monoclinic phase of zirconia. The photoluminescence spectra showed intense blue emission on excitation at 260 nm. The peaks are positioned at 361 nm, 424 nm, 440 nm, 487 nm. These peaks are arising due to oxygen vacancy defects and singly ionized oxygen vacancy in the zirconia lattice. The material also used to develop latent fingerprints, which show clear formation of finger print tracks, justifying that the material is a good competitor in forensic application.

Graphical Abstract



Keywords: Flower like Monoclinic Zirconia, Photoluminescence, Latent Finger Print Studies.

INTRODUCTION

Zirconia is a very good material with its wide spread applications. It is used as a thermal insulating material [1], solid electrolyte in fuel cell [2] and works as an excellent material for catalysis, because of its high surface area [3, 4]. Luminescence (optical property) of different forms of zirconia was studied by a large number of researchers. However, the results of the luminescence study differ. The luminescence observed from zirconia at room temperature will be attributed to the defect states. Formation of these defect states will be significantly influenced by the methods of preparation and material processing protocols. There are many methods reported in the literature for the preparation of metal oxide nano particles like, hydrothermal [5], sol-gel synthesis [6], combustion chemistry [7] and precipitation method [8]. Out of all the methods, precipitation method follows mild and environmentally benign protocol with maximum recovery of the nanomaterial. Hence, we opted precipitation method to synthesis zirconia, the prepared material was characterized for its structural and morphological analysis. The material synthesized was used for its photoluminescence and latent finger print applications.

MATERIALS AND METHODS

Preparation of ZrO_2 nanoparticles by precipitation method: The precipitation method was used in the preparation of ZrO_2 material. In this procedure precipitation of material was carried out under high dilution. In the typical procedure, 32.27 g of $\text{ZrOCl}_2 \cdot 8\text{H}_2\text{O}$ was dissolved in 3L of double distilled water, which was taken in a 5 L beaker, this gives $\text{ZrOCl}_2 \cdot 8\text{H}_2\text{O}$ solution of 0.0333M concentration. Liquor ammonia (25% Merck) was added to the above solution at a constant stirring rate of 1000 rpm at room temperature. The addition was carried over a period of 5 h by regularly monitoring the pH of the solution using calibrated pH meter. The process continued till the pH of the solution reaches 7.5, during this over saturation effect results in complete precipitation of $\text{Zr}(\text{OH})_4$. Stirring was continued for 30 min even after the completion of addition of liquor ammonia. The white precipitate obtained was allowed to age overnight (24 h). The supernatant liquid containing counter ions was decanted and the precipitate was washed with distilled water 5 times. The precipitate was filtered with continuous washings and the filtrate was continuously checked for the presence of chloride ions using silver nitrate solution. Washing was continued till the filtrate gave negative test for chloride ions. Finally, the precipitate was washed with ethyl alcohol three times, thus obtained white precipitate was dried in a hot air oven at 120°C for a period of 7 h. The dried material ground to fine powder, sieved using $90\ \mu$ mesh and subjected to calcination at 400°C in a pre-heated muffle furnace for 4 h. During this process water of hydration gets completely eliminated and gives free flowing ZrO_2 nano material. Thus, obtained material was stored under vacuum desiccator till further usage for its activity studies.

RESULTS AND DISCUSSION

PXRD analysis of prepared ZrO_2 material: The X-ray patterns were recorded for the sample with PANalytical X'pert X-ray diffractometer (PXRD). Phase formation and crystal structure of the ZrO_2 material calcinated at 400°C was studied by XRD analysis with $\text{Cu-K}\alpha$ radiation source having a wavelength of 1.54056\AA . The obtained pattern was shown in figure 1. From the figure it is evident that the material has distinct XRD pattern with 2θ values positioned at 24.13, 28.21, 31.46, 34.19, 35.22, 40.87, 49.34, 55.50 and 59.97 indicating monoclinic structure of ZrO_2 . The data is in good agreement with the crystal data having JCPDS card number 24-1165.

The unit cell parameters of the material were calculated from the most intense diffraction lines gave $a=5.145$ $b=5.207$ $c=5.311$ \AA). The average particle size was calculated using Debye-Scherrer equation $D = K\lambda/\beta\cos\theta$. Where, λ is the wavelength of X-rays, K is crystallite shape factor which was assumed to be 0.90, θ is the diffraction angle and β is the corrected full width at half maximum, the average crystallite size was found to be 80.14 nm. The crystallite size was also calculated by Williamson- Hall method, a detailed calculation followed was presented in table 1.

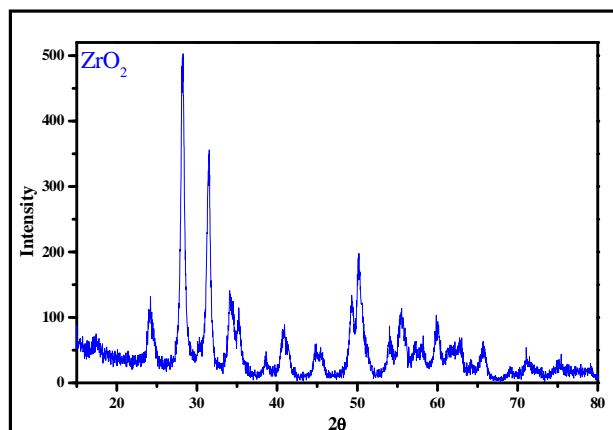


Figure 1. XRD pattern of ZrO_2 material calcinated at 400°C

Table 1. Calculation of average crystallite size of ZrO_2 by Williamson-Hall method

Sl. No.	θ	β	β in rad	$\sin\theta$	$4\sin\theta$	$\beta\cos\theta$
1	12.0658	0.5647	0.00986	0.20906	0.83625	0.00964
2	14.106	0.5966	0.01041	0.24375	0.97499	0.0101
3	15.7312	0.6219	0.01086	0.27116	1.08464	0.01045
4	17.0983	0.8527	0.01488	0.29405	1.1762	0.01423
5	17.613	0.7695	0.01343	0.30262	1.21049	0.0128
6	20.4334	0.9714	0.01696	0.34916	1.39665	0.01589
7	24.6718	1.0195	0.0178	0.41747	1.66988	0.01617

A graph of $4\sin\theta$ and $\beta\cos\theta$ was plotted along x and y axis respectively as shown in figure 2. The slope of the graph provides the strain in the lattice and y-intercept gives the crystallite size as per Williamson-Hall plots. The crystallite size calculated to be 76.60 nm using the relation $\beta\cos\theta = (K\lambda/D) + 4\epsilon\sin\theta$ (Williamson-Hall method). Where, β is the full width at half maximum, k is the shape factor taken as 0.9 for spherical particles and λ is the wavelength of X-rays.

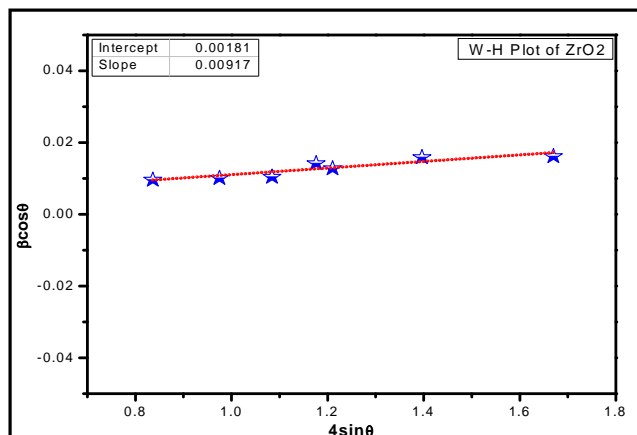


Figure 2. Williamson-Hall plot of ZrO_2

FT-IR characterization of ZrO_2 material: The FTIR spectra of ZrO_2 nanomaterial was recorded in the range of $300\text{--}4000\text{ cm}^{-1}$ using Bruker-Alpha Fourier transform infrared spectrometer. Figure 3

shows the Infrared spectra of ZrO_2 material calcinated at 400°C . Peaks positioned at 361cm^{-1} , 414cm^{-1} and 500cm^{-1} are tetragonal bands. The dominant sharp absorption band centered at 576cm^{-1} is due to the deformation mode bending vibrations of Zr-O-Zr bond [9-11], a sharp band at 749cm^{-1} is the characteristic distinctive band for monoclinic ZrO_2 . The weak peaks centred at 1268cm^{-1} , 1319cm^{-1} can be associated to stretching vibrations of Zr-O terminal/non-bridging atom. Weak band centered at 1628cm^{-1} is attributed to H_2O bending mode. The broad band centered at 3402cm^{-1} may be the result of atmospheric moisture retained by ZrO_2 and is ascribed to the stretching of O-H group of water [12]. These minor changes in the infrared frequency of the sample will be credited to the thermal processing protocols followed during the preparation of the material and as well as on the degree of crystalline nature of the ZrO_2 .

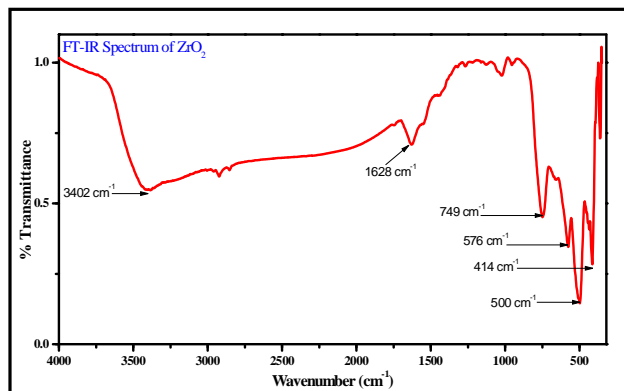


Figure 3. FTIR spectrum of ZrO_2

Photoluminescence study: Photo luminescence spectra were recorded in Agilent Cary Eclipse Spectrofluorometer. Figure 4 shows the photoluminescence emission spectra of ZrO_2 material excited at the wavelength 260 nm. The sample showed emission peaks centered at 361 nm, 424 nm, 440 nm, 487 nm and in addition to these peaks a peak centered at 783 was observed. Since Zr^{4+} itself is non-luminescent in nature, the emission behavior of ZrO_2 is attributed to the non-stoichiometric defects created due to the oxygen vacancies created in the lattice.

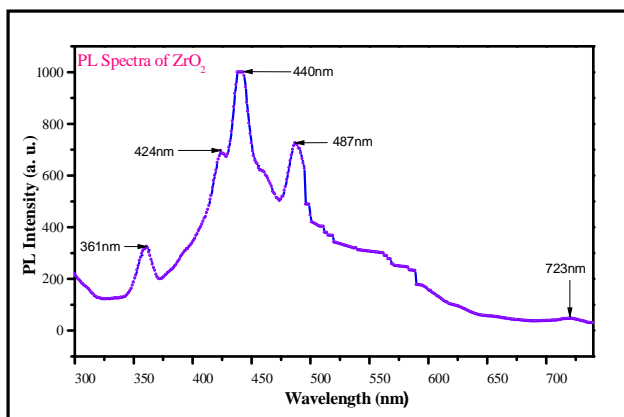


Figure 4. Photo Luminescence spectra of ZrO_2

The emission behavior of ZrO_2 was explained by impurity luminescence center model and structure defect model. Luminescence center model claims that the emission is due to the traces of Ti^{4+} associated with precursor material as obtained. But, as per the Structure defect model, luminescence will be arising due to singly ionized oxygen-vacancies. ZrO_2 was prepared by simple

precipitation method. The XRD, FTIR data clearly confirms the absence of Ti^{4+} and P. Hence, the emission behavior ZrO_2 is purely due to the oxygen-vacancy effect. An appreciable intensive peak at 424 nm is attributed to the singly ionized associated oxygen vacancy defects (AOD^+) centers; the band at 487 nm is due to the additional oxygen vacancies. A peak centered at 723 nm is originating due to the combination emission of electrons and holes in oxygen vacancies of ZrO_2 [13, 14].

The CIE chromaticity coordinates ZrO_2 was calculated, which was shown in figure 5a. The CIE chromaticity graph indicates blue emission by ZrO_2 . It is observed that, the CIE co-ordinates were close to white emission region. CCT was used to define the color temperature of a light source. This is done by determining the temperature of the closest point of the Planckian locus compared to the light source on the (U' , V') uniform chromaticity diagram. The material showed high CCT value as shown in figure 5b.

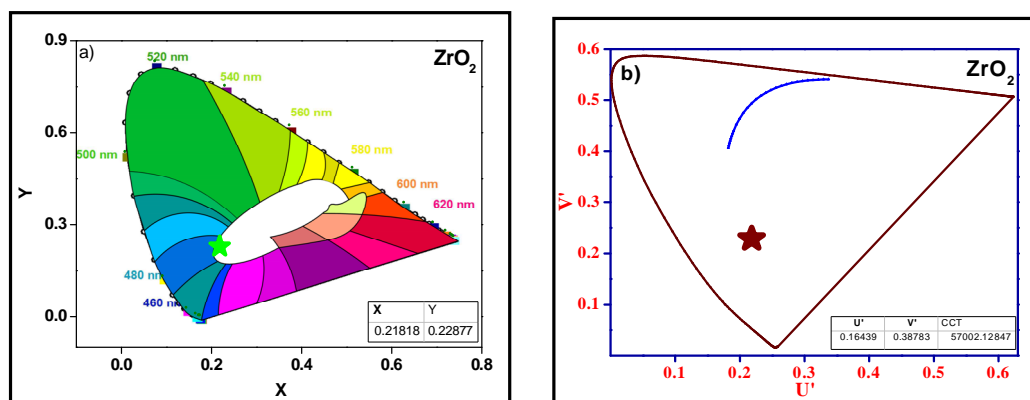


Figure 5. a) CIE chromaticity diagram of ZrO_2 and b) CCT diagram of ZrO_2

FESEM analysis of ZrO_2 : SEM micrographs were recorded using Zeiss field emission scanning electron microscope, the micrographs are as shown in the figure 6 (a-d). The micrographs are recorded at different magnifications as mentioned in the figure. The results reveal that the preparation of the ZrO_2 by the detailed protocol mentioned in the experimental section and subsequent reaction conditions lead to the formation of ZrO_2 nano flowers with marigold flower shape. This was clearly

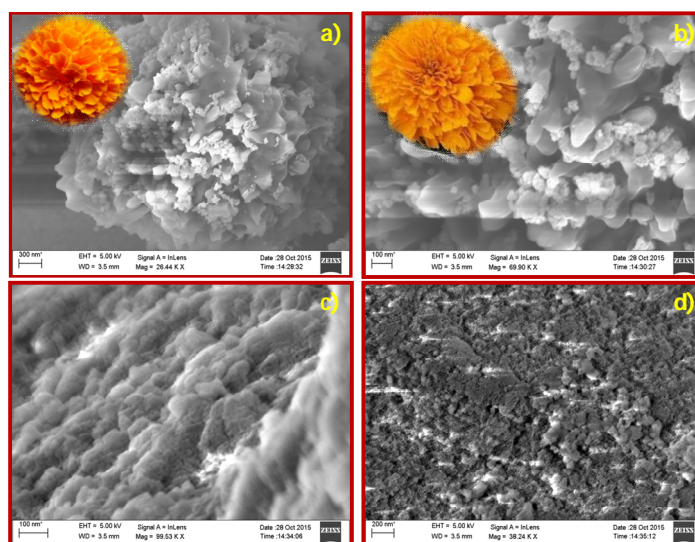


Figure 6. (a to d) FESEM images of ZrO_2 at different magnifications

seen. A comparison of nano ZrO_2 with marigold flower structure was shown in the inset of the micrographs, which were shown in the figures 6a and 6b. The ZrO_2 material has porous structure with high surface area with high agglomeration. These are the specific nature when the materials are prepared by precipitation technique. However, this can be avoided by adding suitable surfactants or structure modifiers. The porous nature may be arising due to the escape of water molecules from the lattice and surface during the course of calcination at 400°C .

Latent finger print application: Figure 7 shows the finger print visualization using ZrO_2 . ZrO_2 is a conventional non-fluorescent powder material to develop latent finger prints. The finger prints were recorded on different surfaces like, plastic scale, aluminium foil, steel spatula and compact disc, good images were developed on all these substrates. In the finger print analysis, before obtaining the finger prints, the hands of the donor are washed with soap, maintained clean and dry without touching anything for ten minutes before screen finger print recording. The finger prints are obtained by applying medium pressure by the donor on the substrate. Once the finger prints are obtained the ZrO_2 material was spread and magnetic brushing was used to develop the tracks and to remove excess powder. The developed fingerprints were studied in visible light and using the Nikon D5300/AF-P DX NIKKOR 18-55 mm f/3.5-5.6G VR lens digital camera. Clear visible tracks were developed effectively, with minimum background disturbance.

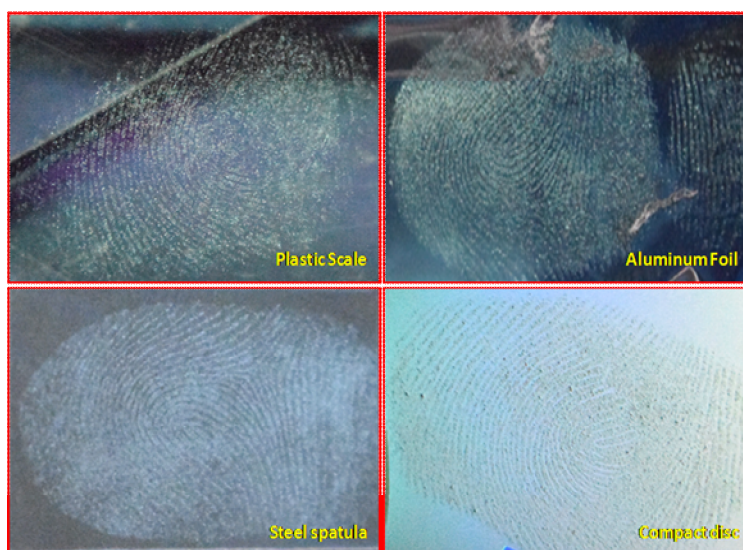


Figure 7. Latent finger print revelation with ZrO_2 nano powder

APPLICATION

The prepared Flowerlike monoclinic zirconia nano powder exhibits blue luminescence under UV excitation. The fine nano powder was used to develop latent finger print images, to demonstrate its utility in forensic applications.

CONCLUSION

In conclusion flower like zirconia nano material was prepared by simple precipitation method. The prepared material was characterized for its structural and morphological features by FTIR, XRD and SEM, the data indicates- porous, flower like, agglomerated zirconia nano material with monoclinic structure. The prepared nano powder exhibited blue luminescence under UV excitation. The fine nano powder was used to develop latent finger print images, to demonstrate its utility in forensic applications.

REFERENCES

- [1]. A. Emeline, G. V. Kataeva, A. S. Litke, A. V. Rudakova, V. K. Ryabchuk, N. Serpone, Spectroscopic and Photoluminescence Studies of a Wide Band Gap Insulating Material: Powdered and Colloidal ZrO_2 Sols. *Langmuir*. **1998**, 14(18), 5011-5022. doi:10.1021/la980083l.
- [2]. J. H. Shim, C. C. Chao, H. Huang, F. B. Prinz. Atomic layer deposition of yttria stabilized zirconia for solid oxide fuel cells. *Chem Mater.*, **2007**, 19(7), 3850-3854. doi:10.1021/cm070913t.
- [3]. L. Parashuram, S. Sreenivasa, S. Akshatha, V.U.Kumar, S. Kumar, Zirconia Supported Cu(I)-Stabilized Copper Oxide Mesoporous Catalyst for the Synthesis of Quinazolinones Under Ambient Conditions, *Asian J Org Chem.*, **2017**, 6(12), 1755-1759. doi:10.1002/ajoc.201700467.
- [4]. G. K. Chuah, S. Jaenicke, B. K. Pong. The preparation of high-surface-area zirconia: II. Influence of precipitating agent and digestion on the morphology and microstructure of hydrous zirconia, *J Catal.*, **1998**, 175(1), 80-92. doi:10.1006/jcat.1998.980.
- [5]. C. J. Szepesi, J. H. Adair, High yield hydrothermal synthesis of nano-scale zirconia and YTZP. *J Am Ceram Soc.*, **2011**, 94(12), 4239-4246. doi:10.1111/j.1551-2916.2011.04806.x.
- [6]. J. M. Carvalho, L. C. V. Rodrigues, M. C. F. C. Felinto, L. A. O. Nunes, J. Hölsä, H. F. Brito. Structure-property relationship of luminescent zirconia nanomaterials obtained by sol-gel method, *J Mater Sci.*, **2014**, 50(2), 873-881. doi:10.1007/s10853-014-8648-7.
- [7]. K. Dhanalakshmi, A. Jagannatha Reddy, D. L. Monika, R. Hari Krishna, L. Parashuram, Concentration dependent luminescence spectral investigation of Sm^{3+} doped Y_2SiO_5 nanophosphor, *J Non Cryst Solids.*, **2017**, 471, 195-201. doi:10.1016/j.jnoncrsol.2017.05.040.
- [8]. F. H. Alhassan, U. Rashid, M. S. Al-Qubaisi, A. Rasedee, Y. H. Taufiq-Yap. The effect of sulfate contents on the surface properties of iron-manganese doped sulfated zirconia catalysts, *Powder Technol.*, **2014**, 253, 809-813. doi:10.1016/j.powtec.2013.12.045.
- [9]. M. Daturi, C. Binet, S. Bernal, J. A. Pérez Omil, J. Claude Lavalley, FTIR study of defects produced in ZrO_2 samples by thermal treatment Residual species into cavities and surface defects, *J. Chem Soc Faraday Trans.*, **1998**, 94(8), 1143-1147. doi:10.1039/a708208h.
- [10]. G. Cerrato, S. Bordiga, S. Barbera, C. Morterra. Surface characterization of monoclinic ZrO_2 . Morphology, FTIR spectral features, and computer modelling, *Appl Surf Sci.*, **1997**, 115(1), 53-65. doi:10.1016/S0169-4332(96)00586-7.
- [11]. A. K. Singh, U. T. Nakate, Properties of Nanocrystalline Zirconia, *Sci J.*, **2014**, 1-7. doi:10.1155/2014/349457.
- [12]. T. Hirata, E. Asari, M. Kitajima, Infrared and Raman Spectroscopic Studies of ZrO_2 Polymorphs Doped with Y_2O_3 or CeO_2 , *J. Solid State Chem.*, **1994**, 110(2), 201-207. doi:10.1006/jssc.1994.1160.
- [13]. K. Smits, D. Olsteins, A. Zolotarjovs, Doped zirconia phase and luminescence dependence on the nature of charge compensation, *Sci Rep.*, **2017**, 7, 1-7. doi:10.1038/srep44453.
- [14]. E. De La Rosa-Cruz, L. A. Díaz-Torres, R. A. Rodríguez-Rojas, M. A. Meneses-Nava, O. Barbosa-García, P. Salas. Luminescence and visible upconversion in nanocrystalline $\text{ZrO}_2:\text{Er}^{3+}$, *Appl Phys Lett.*, **2003**, 83(24), 4903-4905. doi:10.1063/1.1632020.